



Dispersion Characteristics of non-Newtonian fluid during transportation of nanoparticles in permeable capillary

Rekha Bali, Nivedita Gupta and Swati Mishra

Department of Mathematics

HBTI, Kanpur. 208002, India

dr.rekhabali@rediffmail.com; niveditagupta48@gmail.com

Received: April 11, 2016; Accepted: September 3, 2016

Abstract

The present analysis deals with the dispersion characteristics of blood described as Herschel-Bulkley fluid in capillary with permeable walls for fluid and impermeable for the nanoparticles. The contribution of molecular and convective diffusion is recalled from the Taylor and Aris coefficient of diffusion. The effective longitudinal diffusion depends on three parameters namely rheological parameter, pressure parameter, and the permeability parameter. We investigate the influence of the longitudinal transport of nanoparticles with permeable blood vessels on the effective dispersion. It shows that the effective diffusion of nanoparticles reduces with increase in radius of the plug region (i.e., the volume of red blood cells) and the permeability of the blood vessels.

Keywords: Dispersion; Effective longitudinal diffusion; Herschel Bulkley; Fluid; nanoparticles; Rheological parameter

MSC 2010 No.: 76Z05, 76R50

1. Introduction

In nanotechnology, drug delivery has many advantages in several fields: chemical, environmental, and biomedical engineering. The study of nanoparticle development is important because of their double role. They are small enough to be transported with the blood flow but they may be attached to cells and be transported by cells. If they are combined with drugs, these particles may change the transcription processes in cells. Nanoparticles are highly specific, efficient and rapidly internalized by the target cells. Generally, blood is a suspension of cells

such as erythrocytes (red blood cells), monocytes, platelets, proteins etc. About 45% of the blood volume in an average man is occupied by erythrocytes. This fraction is called hematocrit. In small vessels, blood shows a two-phase nature: (i) a peripheral layer of plasma shows Newtonian nature, (ii) a core region of vessel shows non-Newtonian nature. The velocity profile in core region of capillaries can be different from parabolic because of the presence of erythrocytes. For successful delivery, the particles have to pass through the vascular capillary wall. Smaller particles generally circulate longer and are taken up by cells of the lymphatic system and bone marrow while particles greater than 50 nm are taken up by liver cells.

Nanofluids are the fluids of nanometer sized particles of metals, oxides, carbides, nitrides or nanotubes. Nowadays, nanofluids, among researchers, are considered an active area of research. In fact, nanofluids are a suspension of nanosized solid particles in a base fluid. The nanofluids have high thermal conductivity as compared to the base fluid. The longitudinal transport of passive species in a fluid flow is of fundamental importance in different fields as chemical engineering for the transport of reagents, environmental sciences for the transport of pollutants and in bio-nanomechanics for the delivery of nanoparticles carrying therapeutic and imaging agents.

Taylor and Aris (1953 and 1956) proposed an idea of an effective diffusion coefficient D_{eff} and derived it as

$$D_{eff} = D_m + \frac{R_e^2 U^2}{48 D_m},$$

where R_e is the radius of vessel, and U is the mean flow velocity. The D_{eff} accounts for both the diffusive and convective contribution with $P_e = \frac{R_e U}{D_m}$ as the pecelet number. The analysis of Taylor and Aris approach is valid in the limit of large times or long channels and for unidirectional flow. Gill (1967) revisited the Taylor's theory to obtain the local concentration c and derived an expression for D_{eff} . Sharp (1993) derived expressions of D_{eff} for casson fluid model. Decuzzi (2006) obtained a novel and more general expressions of D_{eff} for a Newtonian fluid in a permeable capillary, as

$$D_{eff} = D_m \left[1 + \frac{P_{e_0}^2}{192} f(\Omega, \Pi, z') \right],$$

where P_{e_0} in the pecelet number at the entrance of the capillary ($z' = 0$) and f is the function of the permeability parameter Π and the pressure parameter Ω and of the longitudinal non-dimensional coordinate z' along the capillary. Gentile et al. (2008) analyzed the longitudinal transport of nanoparticles in blood vessels by considering blood as a casson fluid. Further, they analyzed the effect of permeability and the rheology of blood. Shaw et al. (2013) studied drug targeting in a micro vessel with a glycocalyx layer where blood obeys a two phase fluid model. Shaw et al. (2014) studied the dispersion characteristics of blood during nanoparticle assisted drug delivery process through a permeable micro vessel. They investigated the influence of the nanoparticle volume fraction, the permeability of the blood vessels, pressure distribution, yield stress and the radius of the nanoparticle on the effective dispersion.

The object of the present work is to study the longitudinal transport of nanoparticles injected into the blood stream in terms of the effective diffusivity. Here we consider the Herschel- Bulkley fluid model. However, Gentile (2008 and 2010) investigated the longitudinal transport of nanoparticles in blood flow by taking Casson like fluid model. The Herschel – Bulkley equation contains one more parameter than the Casson equation so it would be expected that more detailed information about blood properties can be obtained by designing Herschel- Bulkley fluid model. But none of the authors has derived the effective diffusion coefficient by placing nanoparticle in to the blood as a Herschel Bulkley fluid. Therefore, in the present study, we develop a model on transportation of particles into the blood stream characterized as Herschel Bulkey fluid with an emphasis on the permeability of the capillary and rheology of the blood.

2. Formulation of the Problem

A circular capillary with radius R_e and length l is considered as in Figure 1. A Hershel-Bulkley fluid is considered with capillary walls permeable to the fluid and impermeable to the solute (i.e., nanoparticles).

In the following model, the velocity profile and the mean velocity for a Hershel- Bulkley fluid are expressed in terms of the longitudinal pressure gradient dp/dz . Effective diffusion coefficient D_{eff} depend upon the permeability of the capillary and the rheology of blood i.e., D_{eff} is a function of rheological parameter $\xi_c = \frac{r_c}{R_e}$, the ratio between the plug radius and capillary radius, and of the permeability and pressure parameters Π and Ω , respectively.

2.1. Mean Fluid Velocity for a Herschel-Bulkley fluid

We have considered cylindrical polar coordinate system (r, θ, z) , where r and θ are coordinates along the radial and circumferential directions, respectively; the z -axis is along the axis of the blood vessels, p_0 and p_1 are the inlet and outlet vascular pressures, and π_i is the interstitial fluid pressure.

Here we assumed that, the permeability of the capillary is sufficiently small so that the fluid lateral flux does not modify substantially the velocity profile within the channel, which is parabolic in nature; that is to say, that the lateral fluid flow across the permeable walls affects only the flow rate.

For Herschel-Bulkley fluid the governing equations are

$$\begin{aligned} \tau &= \mu e^n + \tau_0, & \tau &\geq \tau_0, \\ e &= 0, & \tau &< \tau_0, \end{aligned} \quad (1)$$

where

$$e = -\frac{du}{dr}, \quad \tau = \frac{1}{2}Pr,$$

and n is the fluid flow index.

Non-dimensional variables are defined as

$$z' = \frac{z}{l}, \quad p' = \frac{p}{\pi_i}, \quad u' = \frac{u}{u_0}, \quad \mu' = \frac{\mu}{\mu_0}, \quad r' = \frac{r}{R_e}, \quad c' = \frac{c}{c_0}, \quad D_m' = \frac{D_m}{u_0 R_e^2 / l}.$$

In a Herschel-Bulkley fluid, the normalized velocity profile is described by

$$u'(r') = \varphi \left(\frac{P'}{2\mu'} \right)^{\frac{1}{n}} \frac{n}{n+1} \begin{cases} (1 - \xi_c)^{\frac{1}{n}+1}, & r' \leq \xi_c, \\ (1 - \xi_c)^{\frac{1}{n}+1} - (r' - \xi_c)^{\frac{1}{n}+1}, & r' > \xi_c, \end{cases} \quad (2)$$

where

$$\varphi = \frac{R_e}{u_0} \left(\frac{\pi_i R_e}{l \mu_0} \right)^{1/n} \text{ and } P' = \frac{dp'}{dz'}.$$

The volume flow rate is derived by the following formula

$$Q' = 2\pi \int_0^1 u'(r') r' dr', \quad (3)$$

$$Q' = \varphi \left(\frac{P'}{2\mu'} \right)^{\frac{1}{n}} \frac{n}{n+1} A(\xi_c), \quad (4)$$

where

$$A(\xi_c) = (1 - \xi_c)^{\frac{1}{n}+1} \left[1 - \frac{2n}{2n+1} (1 - \xi_c) + \frac{2n}{2n+1} \frac{n}{3n+1} (1 - \xi_c)^2 \right]. \quad (5)$$

The mean fluid velocity is given by

$$U' = \frac{Q'}{\pi} = \varphi \left(\frac{P'}{2\mu'} \right)^{\frac{1}{n}} \frac{n}{n+1} A(\xi_c). \quad (6)$$

2.2. The Pressure Gradient in Permeable Capillary

Decuzzi et al. (2006) defined the differential equation relating the parameters, such as hydraulic conductivity L_p , the interstitial fluid pressure π_i , the inlet and outlet vascular pressures p_0 and p_1 . It can be written as

$$-\frac{\pi R_e^4}{8\mu} \frac{\partial^2 p}{\partial z^2} - L_p (\pi_i - p) \lambda_p = 0, \quad (7)$$

and the non- dimensional form can be given by the equation

$$\frac{\partial^2 p'}{\partial z'^2} - \Pi^2 p' = -\Pi^2, \quad (8)$$

where

$$\Pi = \frac{4l}{R_e} \sqrt{\frac{\mu L_p}{R_e}}, \quad (9)$$

the vascular dimensionless pressure p' is derived as

$$p' = (p_0' - 1)\Omega \cosh \Pi z' + \frac{(p_1' - 1)(1 - \Omega \cosh \Pi)}{\sinh \Pi} \sinh \Pi z' + 1, \quad (10)$$

having pressure parameter

$$\Omega = \frac{p_0' - 1}{p_1' - 1}, \quad (11)$$

and lateral profile of permeable wall is represented by L_p which is equal to $2\pi R_e$. When $z' = 0$, Equation (10) becomes as $p' = (p_0' - 1)\Omega + 1 = p_0'$, the pressure at the inlet being always p_0' ; that is to say, that the inlet pressure does not depend on the parameters Π , Ω , and ξ_c .

The normalized mean velocity for the Herschel-Bulkley fluid flow in a permeable capillary can be derived as

$$U' = \varphi \left(-\frac{1}{2\mu'} \right)^{\frac{1}{n}} \frac{n}{n+1} A(\xi_c) [\Pi(p_1' - 1)]^{1/n} \left[\frac{\cosh \Pi z' - \Omega \cosh (\Pi - z' \Pi)}{\sinh \Pi} \right]^{1/n}; \quad (12)$$

and the normalized mean velocity at the capillary inlet

$$U_0' = \varphi \left(-\frac{1}{2\mu'} \right)^{\frac{1}{n}} \frac{n}{n+1} A(\xi_c) [\Pi(p_1' - 1)]^{1/n} \left[\frac{1 - \Omega \cosh \Pi}{\sinh \Pi} \right]^{1/n}; \quad (13)$$

with the relation

$$U' = \left[\frac{\cosh \Pi z' - \Omega \cosh (\Pi - z' \Pi)}{1 - \Omega \cosh \Pi} \right]^{1/n} U_0'. \quad (14)$$

2.3. Effective Longitudinal Diffusion

The transport of solutes within a concentrated suspension of particles can be augmented due to the effects of shear induced dispersive particle migrations (Gentile et al. 2008, Shaw 2010). The basic idea behind Taylor's approach is that it is not possible to superpose advection and diffusion for a liquid flowing in a pipe under the action of pressure gradient.

The strength of Taylor's approach is to show that a superposition may be done by allowing the particles to move at the average velocity of the fluid and using an effective diffusion coefficient for the particle larger than the usual coefficient derived from the Einstein's formula.

Suppose a capillary tube of radius R_e in which liquid flows at a mean velocity U , carrying particles with a concentration c . The advection-diffusion equation written under a axisymmetric (r, z) form, where z - axis is along the tube's axis of symmetry, is given by

$$\frac{\partial c}{\partial t} + u(r) \frac{\partial c}{\partial z} = \frac{D_m}{r} \frac{\partial}{\partial r} \left(r \frac{\partial c}{\partial r} \right) + D_m \frac{\partial^2 c}{\partial z^2}, \quad (15)$$

where $u(r)$ is the axial velocity of the fluid and $c(r, z, t)$ is the nanoparticle concentration. The term $\frac{\partial^2 c}{\partial z^2}$ in Equation (15) may be omitted if it is assumed that the axial change in concentration is much less than the radial change. Furthermore, we use the transformation $\tilde{z} = z - Ut$, with the auxiliary frame of reference (r, z) moving with the mean velocity U along z . Equation (15) can be written as (Decuzzi et al. 2006, Sharp 1993, Shaw et al. 2014).

$$\hat{u}(r) \frac{\partial c}{\partial \tilde{z}} = \frac{D_m}{r} \frac{\partial}{\partial r} \left(r \frac{\partial c}{\partial r} \right), \quad (16)$$

and the non-dimensional form of above equation is given as

$$\frac{u_0 R_e^2 \hat{u}'}{l D_m} \frac{\partial c'}{\partial \tilde{z}'} = \frac{1}{r'} \frac{\partial}{\partial r'} \left(r' \frac{\partial c'}{\partial r'} \right), \quad (17)$$

where $\hat{u}(r) = u(r) - U$ is the relative velocity about the mean velocity U . The right hand side term defines the molecular diffusion along the radial direction while the left hand side defines longitudinal diffusion owing to the non-uniform radial velocity profile. The nanoparticles are dragged along the capillary by the fluid.

The normalized boundary conditions for the solution of the concentration equation are given by

$$c' = 0 \text{ at } r' = 0, \quad (18)$$

$$\frac{\partial c'}{\partial r'} = 0 \text{ at } r' = 0. \quad (19)$$

Equation (18) shows that the homogeneous boundary condition can be conveniently imposed since D_{eff} is not affected by the value of c' at $r' = 0$ (Decuzzi et al. 2006, Gentile et al. 2008, Sharp 1993, Shaw 2014). Equation (19) follows from the axial symmetry of the problem. It results in

$$c_1'(r') = \phi \frac{r'^2}{4} \left[(1 - \xi_c)^{\frac{1}{n}+2} - \frac{n}{3n+1} (1 - \xi_c)^{\frac{1}{n}+3} \right], \text{ for } r' < \xi_c, \quad (20)$$

where

$$\phi = \frac{u_0 R_e^2}{l D_m} \varphi \left(\frac{P'}{2\mu} \right)^{1/n} \frac{n}{n+1} \frac{2n}{2n+1} \frac{\partial c'}{\partial \tilde{z}'}. \quad (21)$$

Similarly, in the cell-free layer, considering the condition of impermeability of the solute at the walls

$$\frac{\partial c'}{\partial r'} = 0 \text{ at } r' = 1; \quad (22)$$

and the condition of continuity of concentration at the interface $r' = \xi_c$ is given by

$$c' = c_1' = c_2' \text{ at } r' = \xi_c; \quad (23)$$

results in

$$c_2'(r') = \frac{\phi}{2} \left[\left\{ (1 - \xi_c)^{\frac{1}{n}+2} - \frac{n}{3n+1} (1 - \xi_c)^{\frac{1}{n}+3} \right\} \frac{r'^2}{2} - \frac{n}{3n+1} (r' - \xi_c)^{\frac{1}{n}+3} + \left(\frac{n}{3n+1} \right)^2 r'^{\frac{1}{n}+3} - \frac{n}{2n+1} \xi_c r'^{\frac{1}{n}+2} + \frac{2n+1}{n+1} \xi_c^2 \frac{r'^{\frac{1}{n}+1}}{2} + \left\{ \frac{n}{2n+1} - \frac{2n+1}{2(n+1)} - \left(\frac{n}{3n+1} \right)^2 \right\} \xi_c^{\frac{1}{n}+3} \right]. \tag{24}$$

Flux of the solute across a section at fixed \bar{z}' is given by

$$J' = \frac{1}{\pi} \left[\int_0^{\xi_c} (\hat{u}'_c c_1' - D_m' \frac{\partial c_1'}{\partial \bar{z}'}) 2\pi r' dr' + \int_{\xi_c}^1 (\hat{u}'_c c_2' - D_m' \frac{\partial c_2'}{\partial \bar{z}'}) 2\pi r' dr' \right]. \tag{25}$$

From that the ratio of normalized diffusion coefficient and normalized molecular diffusion coefficient is derived by using

$$D'_{eff} = -J' / \frac{\partial c'}{\partial \bar{z}'},$$

as

$$\frac{D'_{eff}}{D_m'} = 1 + P_e^2 \frac{R_e^2}{l^2} \left(\frac{2n}{2n+1} \right)^2 (D + E)Z, \tag{26}$$

where

$$D(\xi_c) = \frac{1}{8} \xi_c^4 \left[(1 - \xi_c)^{\frac{1}{n}+2} - \frac{n}{3n+1} (1 - \xi_c)^{\frac{1}{n}+3} \right]^2, \tag{27}$$

$$\begin{aligned} E(\xi_c) = & \frac{1}{8} (1 - \xi_c)^{\frac{2}{n}+4} + \frac{1}{8} \xi_c^4 (1 - \xi_c)^{\frac{2}{n}+4} - \frac{n}{4(3n+1)} \xi_c^4 (1 - \xi_c)^{\frac{2}{n}+5} \\ & - \left[\frac{1}{8} \left(\frac{n}{3n+1} \right)^2 - \frac{n}{3n+1} \frac{n}{4n+1} - \frac{3}{4} \left(\frac{n}{3n+1} \right)^2 \frac{2n+1}{3n+1} - \frac{1}{4} \left(\frac{n}{3n+1} \right)^2 \frac{2n+1}{5n+2} \right] (1 - \xi_c)^{\frac{2}{n}+6} \\ & - \left[\frac{n}{3n+1} \frac{n}{4n+1} \frac{n}{5n+1} + \left(\frac{n}{3n+1} \right)^2 \frac{n}{4n+1} + \frac{3}{2} \left(\frac{n}{3n+1} \right)^2 \frac{2n+1}{4n+1} \frac{n}{5n+1} + \frac{3}{2} \left(\frac{n}{3n+1} \right)^3 \frac{2n+1}{4n+1} \right] (1 - \xi_c)^{\frac{2}{n}+7} \\ & - \left(\frac{n}{3n+1} \right)^2 \frac{n}{5n+1} (1 - \xi_c)^{\frac{1}{n}+2} + \left[\left(\frac{n}{3n+1} \right)^2 \frac{n}{5n+1} + \frac{1}{2} \left\{ \frac{n}{2n+1} - \frac{2n+1}{2(n+1)} - \frac{n}{(3n+1)^2} \right\} \right] (1 - \xi_c)^{\frac{1}{n}+2} \xi_c^{\frac{1}{n}+5} \\ & + \frac{2n+1}{2(n+1)} \frac{n}{3n+1} (1 - \xi_c)^{\frac{1}{n}+2} \xi_c^{\frac{1}{n}+5} + \frac{n}{3n+1} \frac{n}{4n+1} \xi_c (1 - \xi_c)^{\frac{1}{n}+2} - \frac{n}{3n+1} \frac{n}{4n+1} (1 - \xi_c)^{\frac{1}{n}+2} \xi_c^{\frac{1}{n}+5} \\ & - \frac{2n+1}{2(n+1)} \frac{n}{3n+1} \xi_c^2 (1 - \xi_c)^{\frac{1}{n}+2} + \frac{1}{8} \left(\frac{n}{3n+1} \right)^2 \xi_c^4 (1 - \xi_c)^{\frac{2}{n}+6} \\ & + \left[\left(\frac{n}{3n+1} \right)^2 \frac{n}{4n+1} \frac{n}{5n+1} + \frac{3}{2} \left(\frac{n}{3n+1} \right)^3 \frac{2n+1}{4n+1} \frac{n}{5n+1} \right] (1 - \xi_c)^{\frac{2}{n}+8} \\ & + \left(\frac{n}{3n+1} \right)^3 \frac{n}{5n+1} (1 - \xi_c)^{\frac{1}{n}+3} - \left[\left(\frac{n}{3n+1} \right)^3 \frac{n}{5n+1} - \frac{n}{2n+1} \frac{n}{3n+1} \frac{n}{4n+1} \right] (1 - \xi_c)^{\frac{1}{n}+3} \xi_c^{\frac{1}{n}+5} \\ & - \frac{n}{2n+1} \frac{n}{3n+1} \frac{n}{4n+1} \xi_c (1 - \xi_c)^{\frac{1}{n}+3} + \left(\frac{n}{3n+1} \right)^2 \frac{2n+1}{2(n+1)} \xi_c^2 (1 - \xi_c)^{\frac{1}{n}+3} \end{aligned}$$

$$\begin{aligned}
 & - \left[\left(\frac{n}{3n+1} \right)^2 \frac{2n+1}{2(n+1)} + \frac{1}{2} \left\{ \frac{n}{2n+1} - \frac{2n+1}{2(n+1)} - \left(\frac{n}{3n+1} \right)^2 \right\} \frac{n}{3n+1} \right] (1 - \xi_c)^{\frac{1}{n}+3} \xi_c^{\frac{1}{n}+5} \\
 & - \left[\frac{3}{4} \left(\frac{n}{2n+1} \right) + \frac{2n+1}{2(3n+1)} \frac{n}{5n+2} \right] (1 - \xi_c)^{\frac{1}{n}+5} + \frac{2n+1}{4(3n+1)} \left(\frac{n}{3n+1} \right)^2 \\
 & - \left[\frac{n+1}{5n+2} \frac{2n+1}{2n} \left(\frac{n}{3n+1} \right)^2 + \frac{n}{2(5n+2)} \right] \xi_c + \left[\frac{n+1}{8} \frac{1}{(3n+1)^2} + \frac{n+1}{4(2n+1)} + \frac{1}{8} \frac{2n+1}{n+1} \right] \xi_c^2 \\
 & - \left[\frac{n+1}{4n} \frac{1}{3n+2} + \frac{(2n+1)^2}{4n(3n+2)} \right] \xi_c^3 + \frac{1}{16(n+1)} \left(\frac{2n+1}{n} \right)^2 \xi_c^4 \\
 & - \left[\frac{n+1}{4(2n+1)} - \frac{n}{2(5n+2)} - \frac{n+1}{4n} \frac{1}{3n+2} - \left\{ \frac{n+1}{3n+2} - \frac{n}{2(2n+1)} - \frac{1}{4n} \right\} \frac{(2n+1)^2}{4n(n+1)} \right. \\
 & \left. - \left\{ \frac{n+1}{5n+2} - \frac{n}{2(3n+1)} - \frac{n+1}{4n} \frac{1}{2n+1} \right\} \frac{2n+1}{2n} \left(\frac{n}{3n+1} \right)^2 \right] \xi_c^{\frac{1}{n}+6} \tag{28}
 \end{aligned}$$

$$Z(\xi_c) = \left[1 + \left(\frac{2}{n} + 2 \right) \xi_c \right] \left[1 + \frac{4n}{2n+1} (1 - \xi_c) - \frac{4n}{2n+1} \frac{n}{3n+1} (1 - \xi_c)^2 \right]. \tag{29}$$

Substituting Equation (14), it can be represented as

$$\frac{D'_{eff}}{D'_m} = 1 + P_{e_0}^2 \frac{R_e^2}{l^2} \left(\frac{2n}{2n+1} \right)^2 \left[\frac{\cosh \Pi z' - \Omega \cosh (\Pi - z' \Pi)}{1 - \Omega \cosh \Pi} \right]^{2/n} (D + E) Z, \tag{30}$$

where $P_e = \frac{R_e U}{D_m}$, the peclet number and P_{e_0} is the peclet number at the inlet of the capillary.

3. Results and Discussions

The effect of the governing parameters such as peclet number, pressure distribution, permeability of the capillary and the rheology parameter on the relative effective longitudinal diffusion D'_{eff}/D'_m are shown in Figures 2 - 6. The physical parameters considered for the present study are given in the Table 1. The expression derived for the effective longitudinal diffusion consist of two terms; the first is the molecular diffusion term D'_m and the second depends on the permeability and pressure parameters Π and Ω , respectively with the non-dimensional coordinates z' along the capillary with the rheological parameter ξ_c .

Different sizes of the nanoparticles are used in drug delivery for different organs. The particles greater than 200 nm are efficiently filtered by liver, spleen and bone marrow, while particles smaller than 10 nm can be quickly cleared by the kidneys or through extravasations. Generally, defined as molecules with lengths that range from 1 to 100 nm in at least two dimensions, nanoparticles and nano-sized molecules show remarkable structural diversity and include nano-tubes, dots, wires, fibers and capsules. Nanotechnology has exciting implications for medicine and presents challenges regarding particle biocompatibility. When the nanoparticles are injected into the blood flow, they spread across the vessel under the combined effects of diffusion and fluid flow (Lutters et al. 2004, Singh and Nawla, 2011). In general, as ξ_c increases, the core region of the capillary with a flat velocity grows and reduces the thickness of the lateral cell-free layer. This leads to the enhancement of the volume fraction of RBC in the blood which increases the nanoparticle concentration in vessels thereby leading to higher relative diffusion rate.

The influence of ξ_c on the effective longitudinal transport is shown in Figure 2 where the ratio D'_{eff}/D_m' is plotted for different values of pecelet number for impermeable capillary ($\Pi = 0$). The ratio D'_{eff}/D_m' decreases sharply as ξ_c increases up to 0.4. As ξ_c further increases, there is no change. At fixed ξ_c , D'_{eff}/D_m' increases with increasing pecelet number P_e . For ξ_c tending to unity, the effective diffusion D'_{eff} becomes equal to D_m' (molecular diffusion).

With an increase in the volume fraction of the nanoparticle, the interparticle distance decreases which disturbs the rotational motion of red blood cells. This reduces the nanoparticle motion towards the capillary wall and reduces the relative effective diffusion ratio of the nanoparticles which is shown in Figures 3 - 6. Figure 3 depicts the ratio D'_{eff}/D_m' as a function of the rheological parameter ξ_c in permeable capillary ($\Pi = 2, \Omega = -2, P_{e0} \approx 16$). In this graph, the ratio D'_{eff}/D_m' decreases up to the point 0.6; after that point, this ratio increases. The portion of the capillary where $D'_{eff} = D_m'$ becomes wider as ξ_c increases. Similar results were obtained by Gentile (2008) using Casson fluid model.

Figure 4 shows that the ratio D'_{eff}/D_m' decreases as permeability parameter Π increases ($\Pi = 4$). It is also clear from the figure that the portion of the capillary where $D'_{eff} = D_m'$ becomes wider than in Figure 3. This distance decreases between any two consecutive curves for different values of rheological parameter ξ_c .

In figure 5, the effect of the pressure parameter Ω is detected with permeability parameter $\Pi = 2$ for different values of rheological parameter ξ_c . The ratio D'_{eff}/D_m' changes until the particle diffusion reaches a minimum value at $z' = 0.6$. When z' reaches above 0.6, it gives the portion of the vessel where $D'_{eff} = D_m'$ up to the point 0.8. After that point the ratio D'_{eff}/D_m' further increases. Figure 6 shows that at a fixed ξ_c , the ratio D'_{eff}/D_m' decreases more in comparison to corresponding curve in Figure 5. This is due to the decrease in pressure parameter Π . Thus, as Π is reduced the curves which show the portion of the capillary with $D'_{eff} = D_m'$ move upwards. The velocity profile for the Herschel- Bulkley fluid is shown in Figure 7. It is parabolic in nature and shows that the flat velocity profile increases as the radius of the plug region increases. It means that if there is no RBC, the flow shows Poiseuille character in nature.

4. Conclusions

The effective longitudinal diffusion of nanoparticles injected intravascularly has been estimated for the permeability of the vessel and the rheology of the blood. The effect of the permeability parameter Π , the pressure drop across the vessel wall Ω , the rheological parameter ξ_c has been analyzed. It has been shown that the effective diffusion coefficient reduces as ξ_c and Π increase. From the above findings, we can conclude that, the main strategy is that to increase the number of the nanoparticles targeting or reduce the nanoparticle dispersion to the vessels. Finally, it is important to note that the dispersion of the nanoparticles depends on the nature of the organs. Such findings can be of particular consequence towards understanding the role of nanoparticles delivery on the small vessels for designing and developing of nanomedicine based on drug delivery systems.

REFERENCES

- Aris, R. (1956). On the dispersion of a solute in a fluid flowing through a tube. *Proc. R. Soc. Lond. A* 235(1200), 67-77.
- Decuzzi, P., Causa, F., Ferrari, M., and Netti, P. A. (2006). The effective dispersion of nanovectors within the tumor microvasculature. *Ann. Biomed. Eng.* 34:633-641.
- Gentile F., Ferrari M., Decuzzi P. (2008). The transport of nanoparticles in blood vessels: the effect of vessel permeability and blood rheology. *Ann Biomed. Eng.* 36 (2), 254-261.
- Gentile, F., Decuzzi P. (2010). Time dependent dispersion of nanoparticles in blood vessels. *J. Biomed. Sci. and Eng.* 3, 517-524.
- Gill, W.N. (1967). A note on the solution of transient dispersion problems. *Proc. R. Soc. Lond. A* 298: 335-339.
- Lutters, B.C., Leeuwenburgh, M.A., Appeldoorn, C.C., Molenaar, T.J., Van Berkel, T.J., Biessen, E.A. (2011). Blocking endothelial adhesion molecules: a potential therapeutic strategy to combat atherogenesis. *Curr. Opin. Lipidol.* 15, 545-552.
- Tan J., Thomas A., Liu Y., (2012). Influence of red blood cells on nanoparticle targeted delivery in microcirculation. *Soft Matter* 8 (6), 1934-1946.
- Sharp, M.K. (1993). Shear-augmented dispersion in non-Newtonian fluids. *Ann. Biomed. Eng.* 21: 407-415.
- Shaw, S., Ganguly, S., Sibanda, P., Chakraborty, S. (2014). Dispersion characteristics of blood during nanoparticle assisted drug delivery process through a permeable microvessel. *Microvasc. Res.* 92, 25-33.
- Shaw, S., Murthy, P.V.S.N. (2010). Magnetic drug targeting in the impermeable microvessel with two phase fluid model- non Newtonian characteristics of blood. *Microvasc. Res.* 80, 209-220.
- Shaw, S., Murthy, P.V.S.N., Sibanda, P. (2013). Magnetic drug targeting in permeable microvessel. *Microvasc. Res.* 85, 77-85.
- Singh, R., Nawla, H.S., (2011). Medical applications of nanoparticles in biological imaging, cell labeling, antimicrobial agents, and anticancer nanodrugs. *J. Biomed. Nanotechnol.* 7, 489-503.
- Taylor, G., (1953). Dispersion of soluble matter in solvent flowing slowly through a tube. *Proc. R. Soc. Lond. A* 219(1137):186-203.

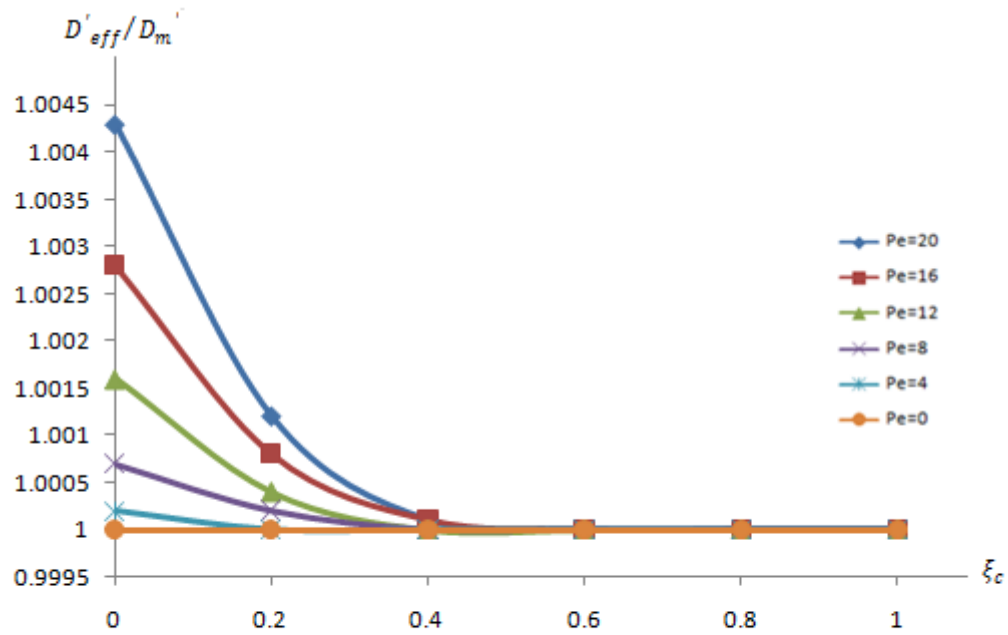
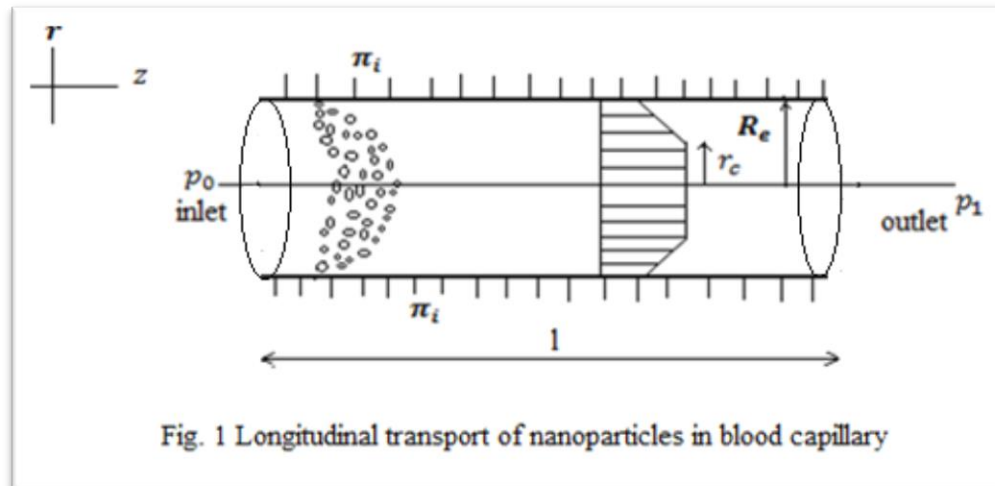


Fig. 2 Variation of D'_{eff}/D_m with ξ_c for different values of peclet number in impermeable capillary

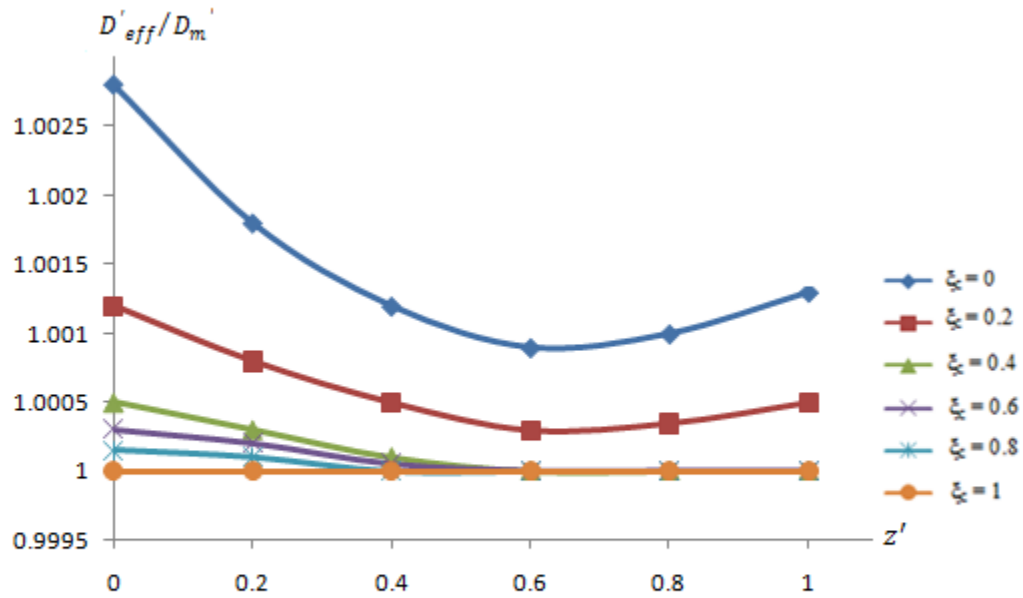


Fig 3. Variation of D'_{eff}/D'_m with z' for different values of ξ_c in permeable capillaries ($\Pi = 2, \Omega = -2, P_{e_0} \simeq 16$).

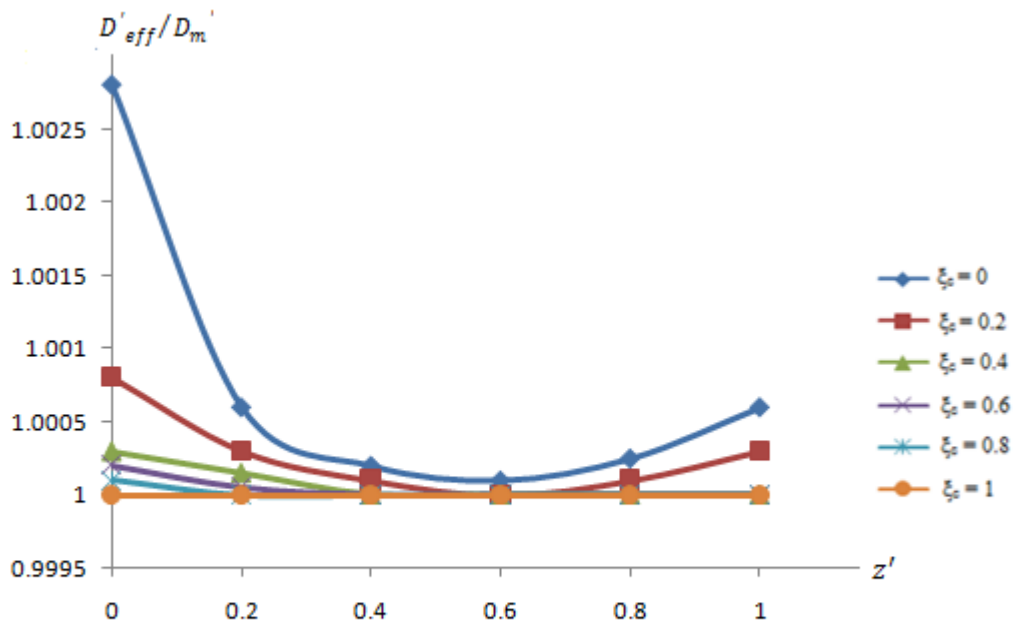


Fig 4. Variation of D'_{eff}/D'_m with z' for different values of ξ_c in permeable capillaries ($\Pi = 4, \Omega = -2, P_{e_0} \simeq 16$).

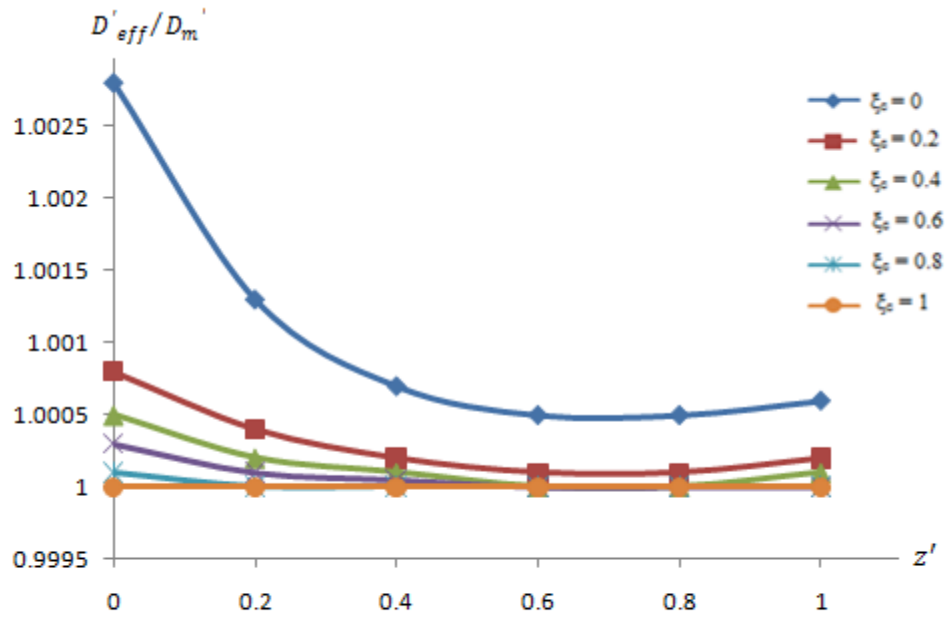


Fig 5. Variation of D'_{eff}/D'_m with z' for different values of ξ_c in permeable capillaries ($\Pi = 2, \Omega = -4, P_{e0} \approx 16$)

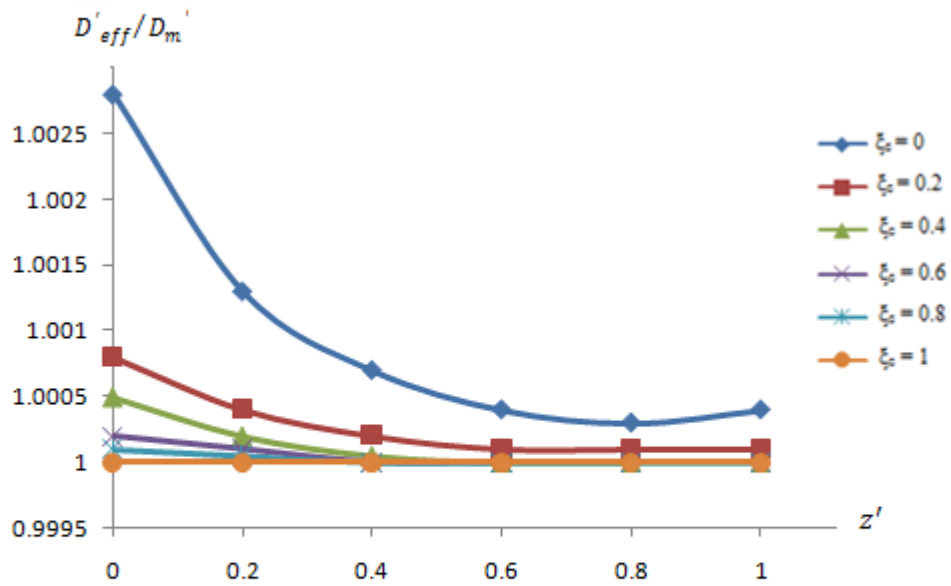


Fig 6. Variation of D'_{eff}/D'_m with z' for different values of ξ_c in permeable capillaries ($\Pi = 2, \Omega = -8, P_{e0} \approx 16$)

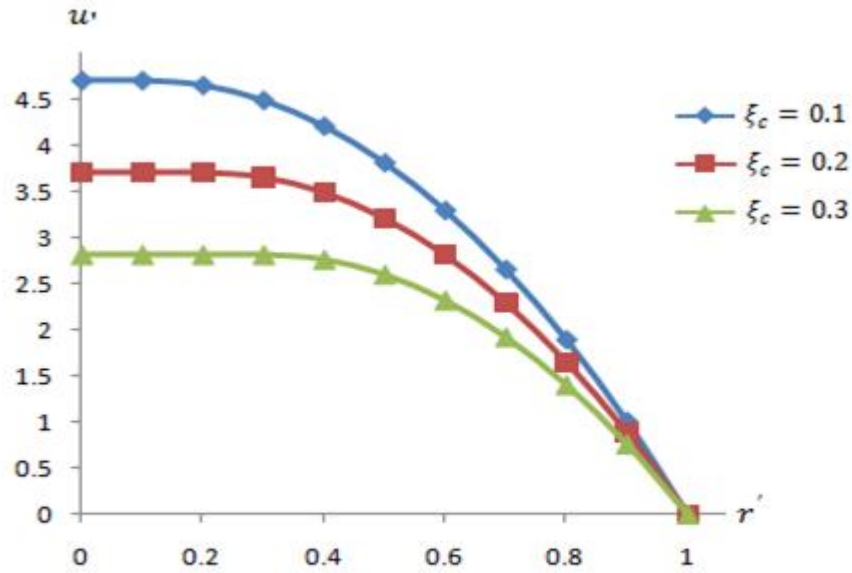


Fig. 7. Velocity profile of Herschel Bulkley fluid in blood capillary

Table 1. Standard values of the parameters

Vessel	R_e (mm)	L(mm)	$P_e = \frac{ReU}{D_m}$	U(mm/s)
Aorta	25	50	1.6×10^{10}	400
Artery	4	1.5-2	6.67×10^8	100
Arteriole	0.02-0.1	1.5-2	$1.67 - 8.33 \times 10^5$	5
Capillary	0.005-0.01	0.5	833- 41667	0.1-1
Venules	0.02-0.05	1	$1.66 - 4.16 \times 10^4$	0.5
Vein	2-5	1-14	$1.6 - 4.1 \times 10^8$	50
Vena Cava	30	40-50	5×10^9	100

P_e is calculated for $D_m = 6 \times 10^{-13} \text{ m}^2/\text{s}$ & flow index of the Herschel - Bulkley fluid (n) = 0.95.